DOI: 10.2478/v10077-011-0006-8

T. Lendze, A. Mielewczyk-Gryń, K. Gdula-Kasica, B. Kusz, M. Gazda
Gdansk University of Technology, Faculty of Applied Physics and Mathematics, Department of Solid State Physics, Gdansk, Poland
e-mail: tlendze@mif.pg.gda.pl

INFLUENCE OF PORE FORMERS ON ELECTRICAL PROPERTIES OF $CaTi_{0.9}Fe_{0.1}O_{3-\delta}$ PEROVSKITE-TYPE CERAMICS

ABSTRACT

Porous $CaTi_{0.9}Fe_{0.1}O_{3-\delta}$ (CTF) perovskites were synthesized by the standard solid state method at different sintering temperatures with carbon black (CB), corn starch (CS) and potato starch (PS) as pore-forming agents. The ceramic samples of porosity between 9% and 42% with 5 - 40 μm pore sizes, were obtained by a 6 h sintering at either 1130º C or 1200º C of precursor powder prepared at 1470º C. X-ray diffraction analysis proved the existence of orthorhombic single-phase perovskites crystalline structure. Electrical conductivity at 800° C was between 1.42×10^{-2} S cm^{-1} and 1.86×10^{-3} Scm^{-1} . The conductivity markedly depended on the sample porosity. It should be noted that 30% of porosity, resulted in reduction of conductivity by less than one order of magnitude. Activation energy of conductivity varied between 0.41 and 0.56 eV. Cornstarch has been chosen as the most suitable pore-forming agent for obtaining the cathode of good properties. The best amount of the cornstarch has been proposed as between 5 and 10%.

Key words: *Proton conductor, perovskite, PCFC, cathode*

INTRODUCTION

Nowadays the interest of hydrogen based energy sources increase rapidly as a clean alternative for traditional fossil fuels (oil, natural gas and coal) [1-4]. Environmentally friendly fuel cells, offer better efficiency than the combustion of hydrocarbons, thanks to chemical energy conversion directly into electricity with a heat as byproduct used for cogeneration. Proton conducting materials allowed to reduce working temperature and elongate lifetime of electrochemical devices, nevertheless a need of physical, chemical and mechanical properties improvement remains a challenge. Among other advantages the possibility of using proton or mixed proton-electron conductors as hydrogen permeable membranes in gas separators should be also mentioned [1].
Electrode materials for Proton Conducting Solid Oxide Fuel Cells (PCFCs), membranes for hydrogen production, oxygen separators and electrolysers should be porous (about 30% porosity is necessary) and should have high protonic and electronic conductivity. Moreover, they should be chemically stable and provide active centers for hydrogen or oxygen gas ionization [5-12]. Simultaneous fulfilling all these conditions is not simple, especially in case of low- and intermediate temperature SOFCs. Therefore, studies of

the relation between the morphology of these materials and their electrical properties are very important.

Chemical stability together with cost effective substrates and manufacturing processes [15] present opportunity for alternative cathode materials, for example iron doped calcium titanates $CaTi_{1-x}Fe_xO_{3-\delta}$ (CTF). The electronic and protonic conductivity of calcium titanate is caused by defect introduced by iron doping. Oxygen vacancies, necessary for protonic conductivity, are created through substitution of Ti^{4+} by lower-valence Fe^{3+} cations:

$$Fe_2O_3 \xrightarrow{2TiO_2} 2Fe'_{Ti} + V_O^{\bullet\bullet} + 3O_O^X \tag{1}$$

Apart from the protonic and electronic conductivity the doped perovskite shows also oxygen-ion conductivity [15-18].

Furthermore the compatibility of the cathode material with the electrolytes and interconnectors is crucial for cathode material. CTF provide reasonable thermal expansion coefficient with regard to known electrolyte ceramics (e.g. TEC of BZY, LSNb and BZCY is 7, 8 and 11×10^{-6} K^{-1}, respectively) [12-14]. For example, M.-L. Fontaine et al. reported TEC of $CaTi_{0.9}Fe_{0.1}O_{3-\delta}$ equal to 10×10^{-6} K^{-1} [12], whereas V. V. Kharton et al. found TEC=12×10^{-6} K^{-1} nearly composition independent [19]. Moreover, calcium titanate has better chemical stability in CO_2, H_2 and is cheaper then other cathode ceramic materials (e.g. LSCF) [12]. Despite known mechanical and chemical advantages of doped calcium titanate at high temperature, the knowledge of their properties at lower temperatures is not sufficient. For instance, the importance of their dependence of electrical properties on micro-structural properties is recognized [16]. Therefore, further studies of this interesting perovskite material are necessary.

In this work powders of $CaTi_{0.9}Fe_{0.1}O_{3-\delta}$ (CTF) perovskites with different porosity and geometry of pores were obtained with the solid-state synthesis. Electrical characteristics in the temperature range applied in the case of intermediate temperature proton solid oxide fuel cells were performed and discussed.

EXPERIMENTAL

Iron-doped calcium titanate $CaTi_{0.9}Fe_{0.1}O_{3-\delta}$ samples were prepared by the solid-state synthesis method. High purity substrates of $CaCO_3$, TiO_2 and Fe_2O_3 in the stoichiometric ratio were mixed and ball milled in ethanol for 12 h. The precursor powders of $CaTi_{0.9}Fe_{0.1}O_{3-\delta}$ were uniaxially pressed (600 MPa) and sintered at 800º C for 20 h. Then, the samples were again milled, pressed and sintered at 1200º C for 12 h and 1470º C for 6 h. Finally, the samples were reground, mixed with the pore former (carbon black, potato- or corn starch) pressed and sintered at either 1130 or 1200º C for 6 h. Sintering was carried out in air atmosphere with heating/cooling rate of 5º C/min at all stages. Porosity was determined using the Archimedes method with a kerosene medium. The phase composition of the synthesized materials was analyzed at room temperature by X-ray diffractometry (XRD) using Cu K_α radiation (λ = 1.5406 Å). The patterns were also analyzed by Rietveld refinement method using a version of the program LHPM1 [20]. As a starting point of the analysis, the crystal structure parameters of $CaTiO_3$ were used [21]. The pseudo-Voigt profile function was applied.

The microstructure of the samples was studied with a Philips-FEI XL 30 ESEM (Environmental Scanning Electron Microscope)**.** The samples containing the desired $CaTi_{0.9}Fe_{0.1}O_{3-\delta}$ perovskite phase with different porosity were chosen for electrical characterization. The DC four-point method was used to examine the samples conductivity. The measurements were carried out at temperature range from 850 K to 1150K and with cooling/heating rate of 5K/min in air. The silver electrodes were deposited by vacuum evaporation onto one side of sample. The wires were attached to the electrodes using silver paste (ESL 4460, ESL Electro-Science).

RESULTS AND DISCUSSION

Figure 1 shows examples of X-ray diffraction spectra of the ceramic samples prepared either without (Fig. 1a) or with the addition of a pore-former (Fig. 1b-d). It can be seen that all the observed XRD reflexes correspond to the perovskite structure. Therefore, regardless the type of applied pore-former, the obtained material is a single-phase $CaTi_{0.9}Fe_{0.1}O_{3-\delta}$ perovskite. Figures 1c and 1d show that there is no influence of prolonging the annealing time from 6 h to 24 h on the composition of the samples containing a pore-former.

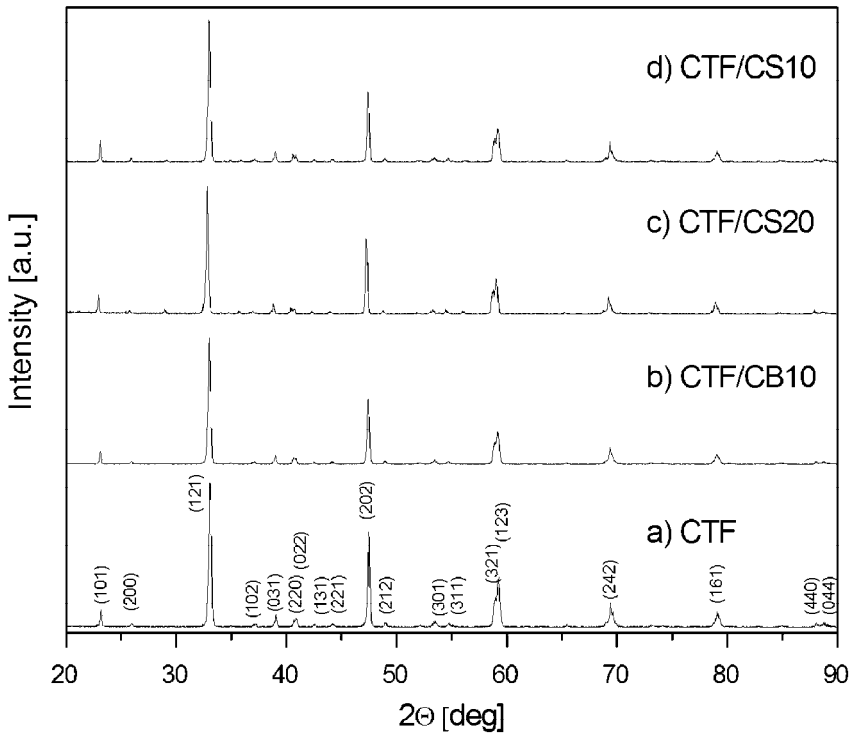

Fig. 1. XRD patterns of the CTF samples. (a) the sample without pore-former, fired at 1470º C for 6 hours; (b) the sample with 10% of carbon black sintered at 1200º C for 6 hours ; (c) the sample with 10% of cornstarch sintered at 1200º C for 24 hours and (d) the sample with 5% of cornstarch sintered at 1130º C for 6 hours

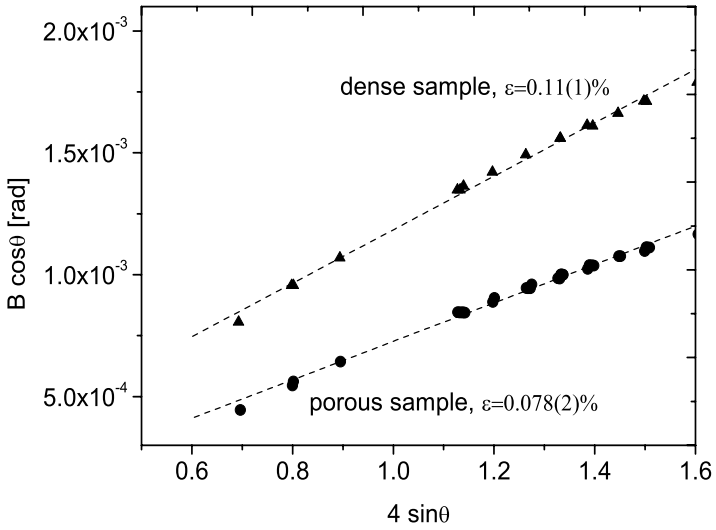

Fig. 2. Williamson-Hall plot of the Bragg reflexes in the dense and porous samples (CTF/CS10, sintered at 1200° C)

X-ray diffraction results, analyzed with the Rietveld method allowed us to determine the unit cell parameters at room temperature. The results are collected in Tab. 1. The differences in the unit cell parameters are rather small, however it may be seen that the volume of the unit cell of the porous samples is smaller than that of the dense one. This difference is probably caused by the presence of rich in carbon pore-formers, which may act as reducing agents. Due to that, larger concentration of oxygen vacancies causing a decrease in the unit cell volume in the porous samples may be expected. Moreover, Rietveld analysis revealed that the X-ray reflexes of the porous samples are of about 10%-30% narrower than these of the dense samples. Main possible sources of the reflex broadening are a crystallite size and residual strain. Taking into account that porous samples were obtained by additional 6 h annealing at 1130 or 1200° C of the ceramic substrates previously prepared by sintering at 1200° C for 20 h and at 1470° C for 6 h, a significant change in crystallite size could not be expected. In order to check a presence of strain, the Williamson-Hall plot of the observed Bragg reflexes has been prepared. The Williamson-Hall plot presented in Fig. 2 shows that the strain present in the porous materials (about 0.08%) is lower than in the dense one (about 0.11%). Therefore, it may be concluded that the residual strain in the porous samples is lower than in the dense ceramics.

Table 1. *Unit cell parameters of the studied samples, obtained with Rietveld refinement method. a,b,c – lattice parameters, V – cell volume*

sample	final sintering temperature (ºC)	space group	a (Å)	b (Å)	c (Å)	V (Å^3)
CTF	1470	*Pnma*	5.4373(2)	7.6474(4)	5.3913(2)	224.179
CTF/CB10	1200	*Pnma*	5.4340(2)	7.6420(3)	5.3866(2)	223.664
CTF/CS20	1200	*Pnma*	5.4351(2)	7.6433(5)	5.3851(2)	223.709
CTF/CS10	1130	*Pnma*	5.4365(2)	7.6429(3)	5.3850(2)	223.749

Figures 3 and 4 show SEM micrographs of dense and porous samples. It can be seen that pore and grain sizes and their distribution depend on both the heat treatment conditions and pore-former addition. Image analysis allowed to estimate average grain and pore sizes. In all cases the grains are not larger than 5-6 μm. In the case of dense samples, the grain size was about 3-5 μm, while the sample with the potato starch consists of grains between 1 and 6 μm. The largest distribution in grain size may be observed in the samples prepared with the addition of carbon and potato starch (Fig. 4). The samples with the cornstarch showed the lowest distribution of the grain size. Moreover, Fig. 3 and 4 show that the pores present in the samples obtained with different pore-formers differ in average size. In all cases there are simultaneously large and small pores present, for example the sample prepared with 10% of corn starch (Fig. 3b) contain the pores between 5-50 μm, while the average pore radius is about 10 μm. Using larger amount of a pore-former leads to an increase of pore size (to 15-40 μm in CS samples), which is shown in Fig.3 b and c. It suggests possible agglomeration of small CS particles during sintering process. The sample obtained with the carbon black seems to be more homogenous than the other samples. The influence of the pore-formers on the sample microstructure results also in different total porosity of the samples. The open porosity and linear shrinkage of the studied samples are collected in Tab. 2. It may be seen that the potato and corn starch addition leads to similar open porosity, while the carbon black is less effective. Porosity increased with the amount of a pore-former and reached about 40%. High temperature of final sintering promotes lower porosity and larger linear shrinkage. All the samples obtained with the addition of pore-formers have the sufficient porosity for application as an electrode for a fuel cell. The samples obtained with the use of cornstarch were less brittle than these made with the addition of potato-starch and carbon black. It is probably caused by more uniform distribution of crystal grain and/or pore sizes.

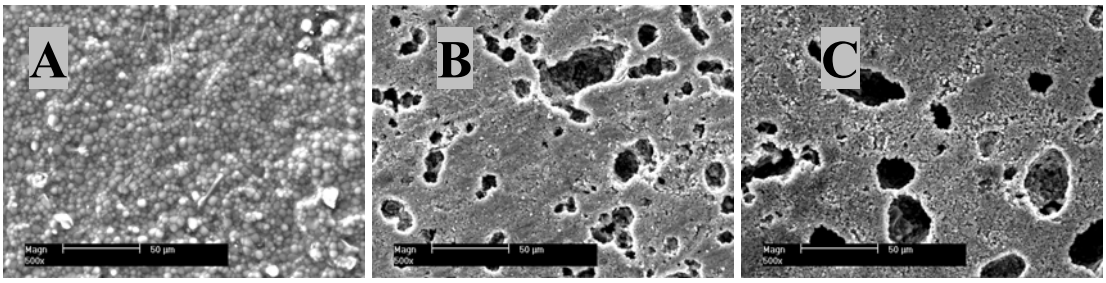

Fig. 3. SEM images obtained for: (a) CTF samples fired at 1470º C (b) CTF sample with 10% of cornstarch fired at 1200º C and (c) CTF sample with 20% of cornstarch fired at 1200º C

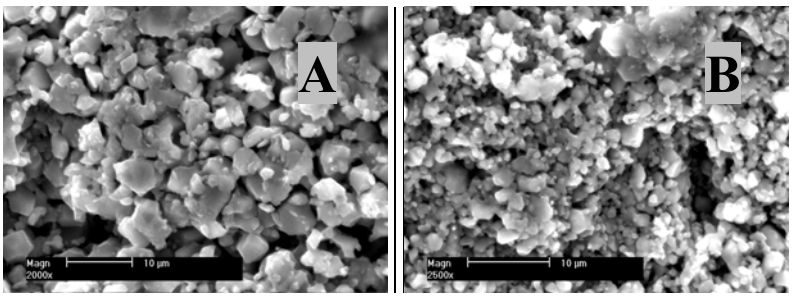

Fig. 4. SEM images obtained for CTF samples: (a) with a 10% of potato starch, and (b) 10% of carbon black

Table 2. *Linear shrinkage, open porosity, total conductivity and activation energy of conductivity of the CTF samples*

sample	final sintering temperature (ºC)	linear shrinkage (%)	open porosity (%)	conductivity at 800 °C (Scm^{-1})	Ea (eV)
CTF	1470	7.9	0.5	$1.42 \cdot 10^{-2}$	0.56
CTF	1200	4.7	9	$8.69 \cdot 10^{-3}$	0.49
CTF	1130	3.1	12	$6.93 \cdot 10^{-3}$	0.41
CTF/CS20	1200	5.8	40	$2.16 \cdot 10^{-3}$	0.46
CTF/CS10	1200	2.8	33	$2.79 \cdot 10^{-3}$	0.53
CTF/CS5	1200	0.6	26	$4.25 \cdot 10^{-3}$	0.44
CTF/CS5	1130	0.5	32	$1.96 \cdot 10^{-3}$	0.45
CTF/PS20	1200	7.0	42	$1.86 \cdot 10^{-3}$	0.44
CTF/CB10	1200	5.9	26	$2.68 \cdot 10^{-3}$	0.45

The temperature dependence of the total conductivity (σ) of the $CaTi_{0.9}Fe_{0.1}O_{3-\delta}$ samples with different pore-formers is shown in Fig. 5. The values of conductivity at 800° C and activation energy of conductivity are also collected in Tab. 2. As it could be expected, the dense sample annealed at 1470° C has the highest conductivity. Lower annealing temperature resulted in higher porosity and lower conductivity. Similar influence of annealing temperature on the conductivity was observed in the case of the samples produced with the addition of pore-formers. It can be seen that the sample containing only 5% of cornstarch annealed at 1130° C shows significantly lower conductivity than the sample annealed at 1200° C. On the other hand, annealing of the samples with pore-formers at temperature higher than 1200° C caused closing of the pores. Therefore, the annealing temperature of 1200° C has been chosen as the optimal one for studying the influence of the pore-formers on the electrical properties. The plots presented in Fig. 5b show that the samples CTF/CS20 and CTF/PS20 of similar porosity (40%) have the lowest conductivity. The CTF/CS10 and CTF/CB10 samples with 33% and 26% of porosity, respectively present slightly higher conductivity. The highest value of conductivity has been observed in the sample CTF/CS5 with 26% of porosity. The comparison of the porosity and conductivity of the samples with carbon black and cornstarch indicates that the cornstarch provides larger porosity accompanied with smaller reduction of conductivity than the carbon. Taking into account its other advantages like better microstructure and mechanical properties, the cornstarch seems to the best pore-former. It should be also noted that 30% of porosity, resulted in reduction of conductivity by less than one order of magnitude. The best amount of the cornstarch, providing sufficient porosity (about 30%) and the largest possible conductivity, may be estimated to be between 5 and 10%

The activation energy of conductivity, calculated on the basis of Arrhenius equation, was about 0.5 eV. No significant correlation of activation energy with the porosity or the type of a pore-former can be found. Nevertheless, the highest value of E_A was obtained for the non-porous sample. Similar results were reported by M.A. Ahmed et al. [16].

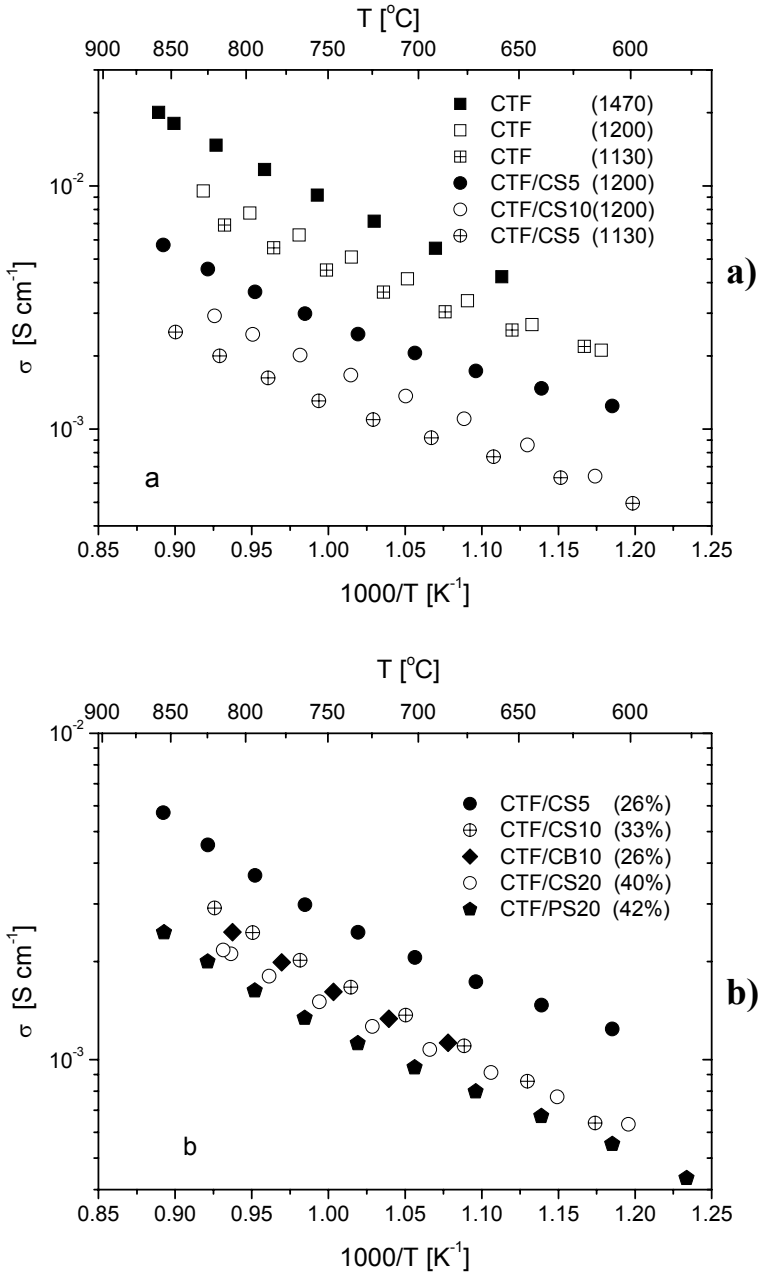

Fig. 5. (a) Temperature dependence of the total conductivity of the dense and porous $CaTi_{0.9}Fe_{0.1}O_{3-\delta}$ samples annealed at various temperatures. (b) Temperature dependence of the total conductivity of the samples obtained with different pore-formers and annealed at 1200° C. Porosity of the samples are given in the parentheses

CONCLUSIONS

In this work porous iron-doped calcium titanate $CaTi_{0.9}Fe_{0.1}O_{3-\delta}$ samples were prepared using carbon black, corn- and potato starch as pore-forming agents. All of them allowed us to obtain porosity sufficient for fuel cell electrode application.

All the porous samples show lower conductivity in comparison to the dense samples. Introduction of pore formers, that provides open porosity about 40% reduces total electrical conductivity by about one order of magnitude. Cornstarch has been chosen as the most suitable pore-forming agent for CTF. The best amount of the cornstarch has been proposed as between 5 and 10%; the larger amount leads to the agglomeration of small CS particles during sintering process.

ACKNOWLEDGEMENTS

The authors would like to thank Jan Stryjewski for the assistance with Environmental Scanning Electron Microscope.

REFERENCES

1. Pasierb P., Drożdż-Cieśla E., Rekas M.: Properties of $BaCe_{1-x}Ti_xO_3$ materials for hydrogen electrochemical separators, Journal of Power Sources 181 (2008), pp. 17–23.
2. Zhu J., Zäch M.: Nanostructured materials for photocatalytic hydrogen production, Current Opinion in Colloid & Interface Science 14 (2009), pp. 260–269.
3. Sahraoui M., Kharrat C., Halouani K.: Two-dimensional modeling of electrochemical and transport phenomena in the porous structures of a PEMFC, International Journal of Hydrogen Energy 34 (2009), pp. 3091 – 3103.
4. Cindrella L., Kannan A.M., Lin J.F., Saminathan K., Ho Y., Lin C.W., Wertz J.: Gas diffusion layer for proton exchange membrane fuel cells-A review, Journal of Power Sources 194 (2009), pp. 146–160.
5. Quarez E., Noirault S., Le Gal La Salle A., Stevens P., Joubert O., Evaluation of $Ba2(In_{0.8}Ti_{0.2})_2O_{5.2-n}(OH)_{2n}$ as a potential electrolyte material for proton-conducting solid oxide fuel cell, Journal of Power Sources 195 (2010), pp. 4923–4927.
6. Bi L., Zhang S., Fang S., Tao Z., Peng R., Liu W.: A novel anode supported $BaCe_{0.7}Ta_{0.1}Y_{0.2}O_{3-\delta}$ electrolyte membrane for proton-conducting solid oxide fuel cell, Electrochemistry Communications 10 (2008), pp. 1598–601.
7. Zhao L., He B., Ling Y., Xun Z., Peng R., Meng G., Liu X.: Cobalt-free oxide $Ba_{0.5}Sr_{0.5}Fe_{0.8}Cu_{0.2}O_3Ld$ for proton-conducting solid oxide fuel cell cathode, International journal of hydrogen energy 35 (2010), pp. 3769 – 3774.
8. Fu X.-Z, Luo J.-L., Sanger A.R., Xu Z.-R., Chuang K.T.: Fabrication of bi-layered proton conducting membrane for hydrocarbon solid oxide fuel cell reactors, Electrochimica Acta 55 (2010), pp. 1145–1149.
9. Matsumoto H., Nomura I., Okada S., Ishihara T.: Intermediate-temperature solid oxide fuel cells using perovskite-type oxide based on barium cerate, Solid State Ionics 179 (2008), pp. 1486–1489.
10. D'Epifanio A., Fabbri E., Di Bartolomeo E., Licoccia S., Traversa E.: Design of $BaZr_{0.8}Y_{0.2}O_{3-\delta}$ Protonic Conductor to Improve the Electrochemical Performance in Intermediate Temperature Solid Oxide Fuel Cells (IT-SOFCs), Fuel Cells 08 (2008), pp. 69–76.
11. Wu T., Peng R., Xia C.: $Sm_{0.5}Sr_{0.5}CoO_{3-\delta}$ –$BaCe_{0.8}Sm_{0.2}O_{3-\delta}$ composite cathodes for proton-conducting solid oxide fuel cells, Solid State Ionics 179 (2008), pp. 1505–1508.

12. Fontaine M.-L., Larring Y., Haugsrud R., Norby T., Wiik K., Bredesen R.: Novel high temperature proton conducting fuel cells: Production of $La_{0.995}Sr_{0.005}NbO_{4-\delta}$ electrolyte thin films and compatible cathode architectures, Journal of Power Sources 188 (2009), pp. 106–113.
13. Yang L., Liu Z., Wang S., Choi Y., Zuo C., Liu M.: A mixed proton, oxygen ion, and electron conducting cathode for SOFCs based on oxide proton conductors, Journal of Power Sources 195 (2010), pp. 471-474.
14. Fontaine M.L., Larring Y., Smith J.B., Raeder H., Andersen Ø.S., Einarsrud M.-A., Wiik K., Bredesen R.: Shaping of advanced asymmetric structures of proton conducting ceramic materials for SOFC and membrane-based process applications, Journal of the European Ceramic Society 29 (2009), pp. 931-935.
15. Figueiredo F.M., Kharton V.V., Waerenborgh J.C., Viskup A.P., Naumovich E.N., Frade J.R.: Influence of Microstructure on the Electrical Properties of Iron-Substituted Calcium Titanate Ceramics, Journal of American Ceramic Society 87 (2004), pp. 2252-2261.
16. Ahmed M.A., Bishay S.T.: Effect of annealing time, weight pressure and Fe doping on the electrical and magnetic behavior of calcium titanate, Materials Chemistry and Physics 114 (2009), pp. 446-450.
17. Shaula A.L., Fuentes R.O., Figueiredo F.M., Kharton V.V., Marques F.M.B., Frade J.R: Grain size effects on oxygen permeation in submicrometric $CaTi_{0.8}Fe_{0.2}O_{3-\delta}$ ceramics obtained by mechanical activation, Journal of the European Ceramic Society 25 (2005), pp. 2613-2616.
18. Figueiredo F.M., Waerenborgh J.C., Kharton V.V., Nafe H., Frade J. R.: On the relationships between structure, oxygen stoichiometry and ionic conductivity of $CaTi_{1-x}Fe_xO_{3-\delta}$ (x = 0.05, 0.20,0.40, 0.60), Solid State Ionics 156 (2003), pp. 371-381.
19. Kharton V.V., Figueiredo F.M., Kovalevsky A.V., Viskup A.P., Naumovich E.N., Jurado J.R., Frade J. R.: The Oxygen Diffusion in, and Thermal Expansion of, $SrTiO3_{3-\delta}$ - and $CaTiO_{3-\delta}$ -Based Materials, Defect Diffusion Forum 186/187 (2000), pp. 119-136.
20. The X'PERT PLUS Rietveld algorithm is based on the source codes of the program LHPM1 (April 11, 1988) of R.J. Hill and C.J. Howard, X'Pert Plus, © 1999 Philips Electronics N.V.
21. Liu, X Liebermann, R C, PCMIDU 20 (1993), 171.